Magnetic and electronic properties of the antiferromagnet $NpCoGa_5$

E. Colineau,[1] P. Javorský,[1,2] P. Boulet,[1] F. Wastin,[1] J. C. Griveau,[1] J. Rebizant,[1] J. P. Sanchez,[1,3] and G. R. Stewart[1,4]
[1]*European Commission, Joint Research Centre, Institute for Transuranium Elements, Postfach 2340, D-76125 Karlsruhe, Germany*
[2]*Charles University, Department of Electronic Structures, Ke Karlovu 5, 12116 Prague 2, The Czech Republic*
[3]*CEA, Département de Recherche Fondamentale sur la Matière Condensée, 38054 Grenoble cedex 9, France*
[4]*Department of Physics, University of Florida, Gainesville, Florida 32611, USA*
(Received 16 December 2003; published 19 May 2004)

The Np counterpart of the superconducting $PuCoGa_5$ compound, $NpCoGa_5$, has been investigated by magnetization, resistivity, specific heat, and ^{237}Np Mössbauer spectroscopy measurements. Unlike the plutonium compound, $NpCoGa_5$ does not show any hint of superconductivity down to $T=0.4$ K but the onset of antiferromagnetic order below $T_N=47$ K. The magnetization experiments evidence a metamagnetic-like transition ($B_c=4.5$ T at $T=5$ K) towards a canted antiferromagnet. The electronic effective mass in $NpCoGa_5$ is moderately enhanced with a Sommerfeld specific heat coefficient $\gamma=64$ mJ mol^{-1} K^{-2}, comparable to that of $PuCoGa_5$. An ordered Np moment of 0.84 μ_B and the occurrence of a Np^{3+} charge state were inferred from the Mössbauer data. Comparison with $NpGa_3$ suggests a moderate delocalization of the $5f$ electrons in $NpCoGa_5$. Similarities and differences with the isostructural $PuCoGa_5$ and $CeMIn_5$ compounds are discussed.

DOI: 10.1103/PhysRevB.69.184411 PACS number(s): 75.30.−m, 71.27.+a, 74.10.+v, 76.80.+y

I. INTRODUCTION

Superconductivity is fascinating as a macroscopic manifestation of a quantum effect, as well as due to its remarkable properties of infinite electrical conductivity and perfect diamagnetism. The observation of unconventional superconductivity in the heavy fermion $CeCu_2Si_2$ in 1979[1] and more recently in antiferromagnets[2,3] and even ferromagnets[4,5] has questioned the BCS theory[6] and revealed the interplay between magnetism and superconductivity. The recent discovery of superconductivity in Pu-based systems[7,8] with critical temperatures one order of magnitude higher than the maximum seen in U and Ce-based heavy fermion systems has opened new perspectives in the chemistry and physics of transuranium compounds, positioning actinide materials as a possible emerging new class of superconductors. A common feature in the physics of all these unconventional superconductors is their proximity to a quantum critical point (which makes it possible to tune these materials, via pressure or chemical substitution, from superconductors to ordered magnets or vice versa) and the idea that superconductivity may be mediated by spin fluctuations. A detailed understanding of the magnetism is crucial to understand its interplay with superconductivity.

$PuCoGa_5$ is a Curie–Weiss paramagnet close to a magnetic instability[9] and exhibits bulk superconductivity below $T_c=18.5$ K,[7] whereas the Pauli paramagnet $UCoGa_5$ is not a superconductor.[10] From the general trends observed in actinide intermetallics, the neptunium counterpart $NpCoGa_5$ is expected to display a stronger magnetic character. In the framework of the search for new transuranium systems and a better understanding of the interplay between magnetism and superconductivity, we have investigated the magnetic and electronic properties of $NpCoGa_5$ using SQUID magnetometry, electrical resistivity, specific heat, and ^{237}Np Mössbauer measurements. Magnetic fields up to $B=9\,T$ and pressures up to $p=7$ GPa have been applied to observe their impact on the physical behavior of $NpCoGa_5$.

II. EXPERIMENTAL

A polycrystalline ingot was obtained by arc melting stoichiometric amounts of the constituent elements under an atmosphere of high purity argon on a water-cooled copper hearth, using a Zr getter. Starting materials were used in the form of 3N8 cobalt and 3N7 gallium shot as supplied by A. D. Mackay Inc., and 3N neptunium metal. Homogeneity of the sample was ensured by turning over and remelting the button several times. Weight losses were below 0.5%.

Single crystals suitable for crystal structure determination were obtained on annealed samples but also on the as-cast samples indicating a congruent formation for this phase. The lattice constants, determined from least square analysis of the setting angles of 25 x-ray reflections, confirmed the tetragonal unit cell and are similar to those determined by x-ray powder diffraction (see below). The x-ray diffraction intensities collected on an Enraf-Nonius CAD-4 four circle diffractometer using a monochromatic Mo $K_{\alpha 1}$ radiation were corrected for Lorentz and polarization effects, and an absorption correction was applied using the psiscans method. Examination of the systematic extinction confirmed that $NpCoGa_5$ crystallizes in the P4/mmm space group (No. 123). The data processing using the Molen package[11] confirmed the $HoCoGa_5$ type ($R=0.036$ and $R_w=0.047$). The phase purity of the sample was checked by x-ray powder diffraction data (Cu K_α radiation) collected on a Bragg-Brentano Siemens D500 diffractometer using a 2θ step size of 0.02 degrees. The diffraction patterns were analyzed by a Rietveld-type profile refinement method using the Fullprof program.[12] The nonannealed sample shows the formation of secondary Np_2CoGa_8-like phase. After subsequent annealing at 750 °C for 2 weeks the sample was found to be pure without any detectable trace of the secondary phase. In agreement with the single crystal study, $NpCoGa_5$ was found to crystallize with the $HoCoGa_5$ structure type with the residual factors $R_B=0.086$ and $R_w=0.06$. The refined structural param-

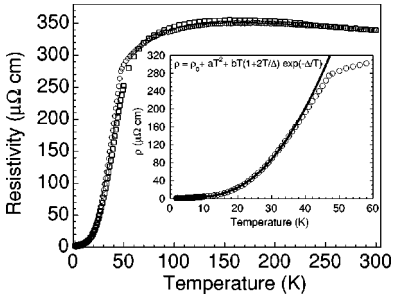

FIG. 1. Electrical resistivity of $NpCoGa_5$ versus temperature at $B=0$ (circles) and $B=9\,T$ (squares). The insert shows the low-temperature fit of $\rho(B=0)$ (see text).

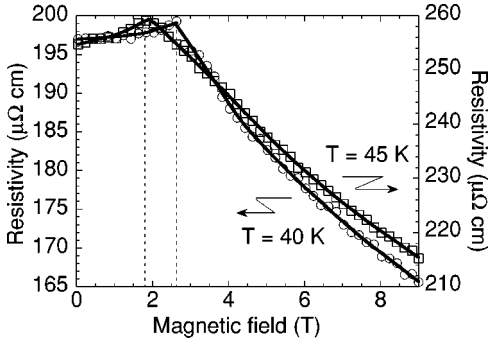

FIG. 2. Resistivity of $NpCoGa_5$ versus magnetic field at $T=40$ K and $T=45$ K.

eters are $a=4.2377(1)$ Å, $c=6.7871(3)$ Å and $z_{Ga}=0.3103(4)$.

DC-magnetization measurements of $NpCoGa_5$ were carried out on a Quantum Design-SQUID magnetometer (MPMS-7) in magnetic fields up to 7 T on a 47 mg piece of polycrystalline sample. The specific heat experiments were performed using a 4 mg $NpCoGa_5$ (14 mg $UCoGa_5$) polycrystalline sample by the relaxation method in a Quantum Design PPMS-9 within the temperature range 0.8–300 K and in magnetic fields up to 9 T. The electrical resistivity was measured on the PPMS-9 system by an AC-four-probe technique on a $1.3\times2.0\times0.8$ mm^3 bulk sample, and in applied fields up to 9 T. High-pressure resistance measurements[13] were carried out by a dc four-probe technique on a $450\times75\times40$ μm^3 platelet sample taken from the ingot, where excitation currents were applied in the basal plane. The ^{237}Np Mössbauer measurements were performed using a sinusoidal drive motion of a ^{241}Am metal source kept at 4.2 K. The temperature of the absorber containing 104 mg Np/cm^2 was varied from 4.2 K to 60 K. The velocity scale of the spectrometer was calibrated with reference to a $NpAl_2$ absorber ($B_{hf}=330\,T$ at 4.2 K).

III. RESULTS

A. Resistivity and resistance under pressure

The resistivity of $NpCoGa_5$ (Fig. 1) is essentially invariant from $T=300$ K down to $T\approx80$ K with a broad maximum around $T\approx170$ K indicative of a Kondo-type behavior. The relatively high resistivity value points to a narrow $5f$ band intersected by the Fermi energy, as confirmed by recent band-structure calculations.[14] Below 80 K, the resistivity decreases significantly and a kink followed by a sharp decrease (see Fig. 1 inset) indicates the onset of a magnetic ordering at $T_N=47.0(5)$ K. No superconducting transition is detected down to the lowest temperature achieved, $T\approx1.8$ K. However, one should note the extremely low residual resistivity, $\rho_0\approx1\,\mu\Omega$ cm, and consequently the extremely high $\rho_{300\,K}/\rho_0$—unusual in the case of a bulk polycrystalline sample.

Below $T\approx37$ K, the resistivity can be accounted for by the law established for antiferromagnetic interactions with the opening of a magnetic gap[15] (insert of Fig. 1):

$$\rho(T)=\rho_0+aT^2+bT(1+2T/\Delta)\exp(-\Delta/T) \qquad (1)$$

with $\rho_0=1.06\,\mu\Omega$ cm, $a=0.0226\,\mu\Omega\,\mathrm{cm\,K^{-2}}$, $b=6.79\,\mu\Omega\,\mathrm{cm\,K^{-1}}$ and $\Delta=55$ K (comparable to T_N). By applying the Kadowaki–Woods relation,[16]

$$a/\gamma^2=\mathrm{const}\sim10^{-5}\ \ \mu\Omega\,\mathrm{cm\,mJ^{-2}\,mol^2\,K^2}; \qquad (2)$$

this value of "a" implies $\gamma\sim48\,\mathrm{mJ\,mol^{-1}\,K^{-2}}$, in good agreement with the value obtained from specific heat (see Sec. III C).

Resistivity measurements were also performed in applied magnetic fields up to 9 T (Fig. 1). At $B=9\,T$, the values obtained from the low-temperature $\rho(T)$ fits slightly decrease compared to zero-field data: $a=0.0201\,\mu\Omega\,\mathrm{cm\,K^{-2}}$ ($\gamma\sim45\,\mathrm{mJ\,mol^{-1}\,K^{-2}}$) and $\Delta=52$ K. With increasing magnetic field the kink at T_N is not shifted but progressively smoothed. In the ordered phase, the field dependence of the resistivity (Fig. 2) shows two distinct regimes suggesting a change of magnetic ordering. Indeed, the resistivity breakdown separating the two regimes indicates the occurrence of a metamagnetic-like transition induced by a critical field ($B_c\sim2\,T$ at $T=40$ K). The resistivity continuously decreases with increasing field above B_c and the highest field applicable, 9 T, is not sufficient to reach a minimum resistivity value.

Electrical resistance was measured under pressure up to 7 GPa and down to 0.4 K. The low pressure measurement shows the same behavior as the zero-pressure resistance curve (Fig. 3). A Kondo-like maximum around 160 K and then a collapse at $T_N=47.0(5)$ K are observed. No hint of a superconducting transition is detected down to 0.4 K. At low pressure the RRR ratio ($R_{300\,K}/R_{1.5\,K}$) is still very high (~80) which confirms the high purity of the sample and the global behavior observed at ambient pressure. With increasing pressure, the RRR decreases from 80 to 15. This decrease does not necessarily reflect a change in the physics of the system but can be due to slight modifications of the form factor under pressure, or of the pressure conditions from hydrostatic ($p\sim2$ GPa) to quasi hydrostatic ($p>3$ GPa). At all applied pressures, the normalized curves ($R(T)/R_{300\,K}$) do not show dramatic change of shape, and the Kondo-like maximum (T_{max}) followed by collapse of resistance below T_N is still observed and becomes sharper as the pressure increases. The evolution of these characteristic temperatures

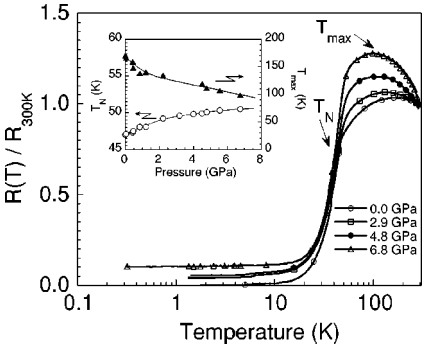

FIG. 3. Normalized resistance curves $R(T)/R_{300\,\mathrm{K}}$ of $NpCoGa_5$ at several pressure points and evolution of the Kondo-like maximum temperature $T_{\max}$ and T_N with pressure (insert).

with pressure (Fig. 3, insert) consists of a substantial decrease of $T_{\max}$ (~ -5 K/GPa), and a simultaneous increase of T_N ($\sim +0.4$ K/GPa) towards a maximum around 51 K. This opposite evolution of $T_{\max}$ and T_N indicates a reinforcement of the magnetic interactions in $NpCoGa_5$ with pressure.

B. Magnetization

At $B=1\,T$, the magnetization as a function of temperature shows a typical antiferromagnetic transition at $T_N=47.0(5)$ K (Fig. 4). At higher fields, the shape of the transition changes considerably, indicating a concomitant change of the magnetic ordering. The evolution of the transition is very progressive. The peak is broadened and shifted to lower temperatures, and at the maximum available experimental field of $B=7\,T$, the curve resembles a ferromagnetic-like transition. However, the maximum magnetization barely reaches $M=0.34\,\mu_B$/Np. The magnetization as a function of the magnetic field clearly shows a transition (Fig. 5) from pure antiferromagnetic order towards ferromagnetic-like order. At $B=7\,T$, the magnetization of $NpCoGa_5$ is still far from saturation and significantly below the value of $0.84\,\mu_B$/Np deduced from the Mössbauer measurements (see Sec. III D). The critical field of this transition varies only little between 5 K and 30 K, from $B_c(5\,\mathrm{K})=4.5\,T$ down to $B_c(30\,\mathrm{K})=3.7\,T$. It then falls rapidly to $B_c=1.7\,T$ at $T=45$ K. However, it is unlikely to be a transition to a pure

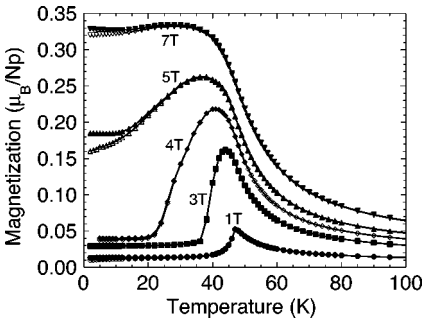

FIG. 4. Zero-field cooled (open symbols) and field-cooled (full symbols) magnetization of $NpCoGa_5$ versus temperature for $1\,T \leqslant B \leqslant 7\,T$.

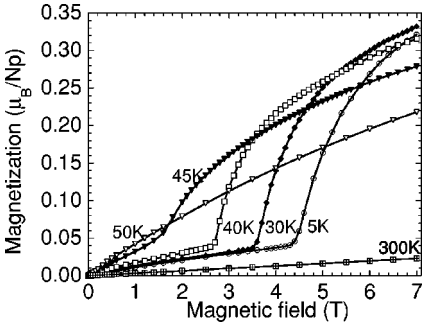

FIG. 5. Magnetization of $NpCoGa_5$ versus magnetic field at various temperatures.

ferromagnetic order since no significant difference is observed on the hysteresis loop between field-up and field-down measurements.

In the paramagnetic state, the magnetic susceptibility obeys a modified Curie–Weiss law:

$$\chi=\chi_0+C/(T-\theta_p). \tag{3}$$

with a positive paramagnetic Curie temperature $\theta_p \approx 42$ K indicative of the presence of ferromagnetic interactions, a reduced effective moment $\mu_{\mathrm{eff}} \approx 1.5\,\mu_B$ [compared to the free ion values, $2.75\,\mu_B(Np^{3+})$ and $3.68\,\mu_B(Np^{4+})$] and a relatively high constant term $\chi_0 \approx 820\times 10^{-6}$ emu/mol. The reduced effective moment could be, at least in part, attributed to the Kondo effect suggested by resistivity measurements, or (and) to crystal field effects.

Finally, no hint of a superconducting transition is detected in the magnetization of $NpCoGa_5$, down to the lowest achieved temperature ($T \approx 2$ K), in agreement with resistivity data.

These results have been obtained on a bulk sample that can substantially differ from an ideal polycrystal. In order to check possible magnetocrystalline anisotropy, we have measured the magnetization of our parallelepipedic bulk sample with field applied along three main directions, denoted I, II, and III (Fig. 6). In the paramagnetic and antiferromagnetic phases, the magnetization remains independent of the orien-

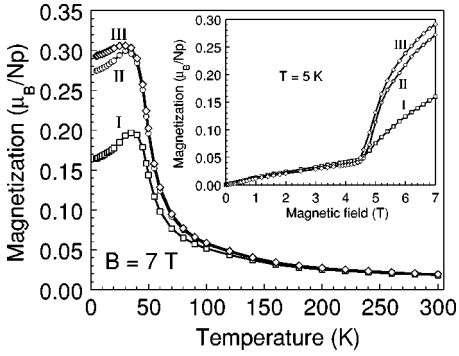

FIG. 6. Magnetization of $NpCoGa_5$ versus temperature at $B=7\,T$ and magnetic field at $T=5$ K (insert) along three main directions of a parallelepipedic bulk sample. The direction I (squares) is taken along the length of the bulk, II (circles) along the thickness (perpendicular to the surface), and III (diamonds) along the width.

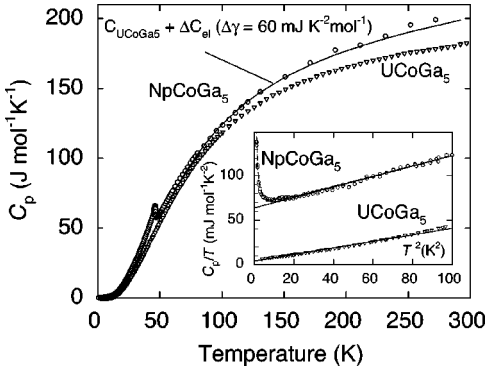

FIG. 7. Specific heat of $NpCoGa_5$ and $UCoGa_5$. ΔC_{el} stands for $\Delta\gamma T$ where $\Delta\gamma$ is the difference between the γ-values for $NpCoGa_5$ and $UCoGa_5$ obtained at low temperature. Insert shows the low-temperature data used to determine the γ-values. The dashed line at very low temperatures includes a term due to the splitting of the ^{237}Np nuclear ground level ($B_{hf}=180\ T$).

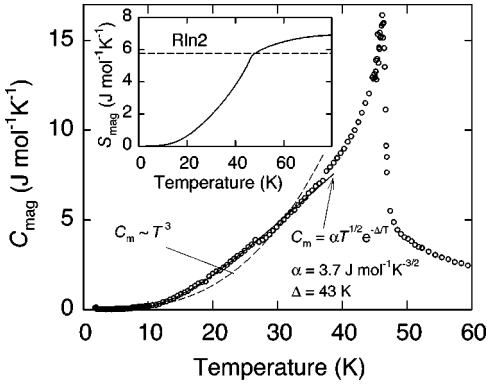

FIG. 8. Magnetic specific heat obtained as $C_m = C_p(NpCoGa_5) - C_p(UCoGa_5) - \Delta\gamma T$. The full line is a fit to the data below 37 K using formula (6). Insert shows the magnetic entropy.

tation. In the ''ferromagnetic'' phase, the magnetization along two directions (II and III) does not display noticeable difference whereas along the third orientation (I) it amounts to only half. This rough experiment, which will be extended once single crystals are available, confirms that $NpCoGa_5$ shows a significant anisotropy and that the crystallites in our bulk sample display preferential orientation. However, the directional independence of the general nature of the intrinsic magnetic behavior in field and temperature discussed above is corroborated.

C. Specific heat

The specific heat of $NpCoGa_5$ is represented in Fig. 7. The magnetic ordering is indicated by a well pronounced anomaly at $T_N = 46.5(5)$ K, in agreement with magnetization and resistivity data.

The specific heat is generally assessed by three contributions: the lattice (phonon) specific heat C_{ph}, the electronic part C_{el} and the magnetic specific heat C_{mag}:

$$C_p = C_{ph} + C_{el} + C_{mag}. \tag{4}$$

To evaluate the magnetic term that is of our main interest, one has first to estimate C_{ph} and C_{el}. At low temperatures, the phonon part can be approximated by a T^3 law and we obtain

$$C_{el} + C_{ph} = \gamma T + \beta T^3. \tag{5}$$

As can be seen from the C_p/T vs. T^2 plot (insert of Fig. 7), our data can be fit to such dependence between 4.5 and 10 K. The magnetic term can also contribute to the specific heat in this temperature region and would influence mainly the slope of the observed dependence. We cannot thus relate the β obtained from the fit exclusively to phonons, but the γ coefficient characterizing the electronic contribution can be estimated with reasonable precision: $\gamma = 64(4)$ mJ mol^{-1} K^{-2}, comparable with the value inferred from the resistivity data above. Below 4.5 K, we notice an increase of the C_p/T data that was not considered in this fit. The origin of the increase of C_p/T can be explained as arising from a nuclear hyperfine Schottky term due to the splitting of the nuclear ground state level ($I=\frac{5}{2}$) of the ^{237}Np nuclei by the hyperfine field reported below.

To determine the lattice contribution, one often takes data of some nonmagnetic equivalent compound. In our case, we can use the paramagnetic isostructural $UCoGa_5$. Its specific heat, shown in Fig. 7, consists of the electronic and lattice part only. The fit of the data to Eq. (5) below 8 K gives the value of $\gamma = 4$ mJ mol^{-1} K^{-2}. Assuming that the phonon contribution is similar in both compounds, the magnetic specific heat of $NpCoGa_5$ can be simply estimated by subtracting the $UCoGa_5$ data and a term ($\Delta\gamma^* T$) that describes the different electronic contribution ($\Delta\gamma = 60$ mJ mol^{-1} K^{-2} is the difference of γ-values of $NpCoGa_5$ and $UCoGa_5$, respectively). This assumption about the phonon contribution is corroborated by the fact that the sum of the $UCoGa_5$ data and ($\Delta\gamma^* T$) term describes quite well the specific heat of $NpCoGa_5$ well above T_N (see Fig. 7) where C_{mag} is assumed to be zero. (Small differences can occur as the lattice is not exactly the same.) Inspecting the data in Fig. 7 indicates that the γ-value in $NpCoGa_5$ is roughly the same in the paramagnetic region and below T_N.

The magnetic contribution extracted this way is represented in Fig. 8. Its approximation at low temperatures by a T^3 dependence, describing antiferromagnetic magnon fluctuations, clearly fails. Instead, it can be well fitted by the formula

$$C_{mag} = \alpha T^{1/2} \exp(-\Delta/T) \tag{6}$$

that describes the specific heat of magnons with an energy gap Δ in their dispersion relation.[17] The fit of C_{mag} up to 37 K, as for the resistivity, gives the values of $\alpha = 3.7$ J mol^{-1} K$^{-3/2}$ and $\Delta = 43$ K.

The integration of C_{mag}/T gives a magnetic entropy of $S_{mag} = 5.6$ J K^{-1} mol^{-1} at T_N, which is close to $R \ln 2$ (= 5.76), the value expected for a doublet ground state. The entropy further increases up to 70 K where it reaches $\approx$6.7 J K^{-1} mol^{-1} and stays more or less unchanged at higher temperatures (insert of Fig. 8). The positive C_{mag}/T above T_N up

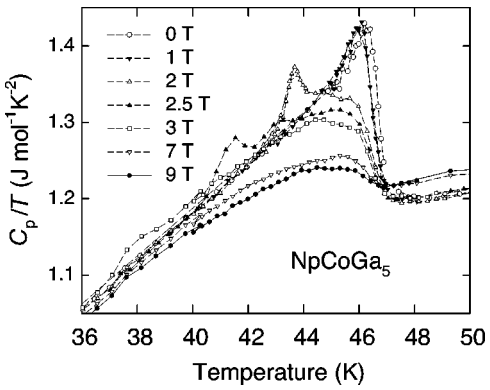

FIG. 9. Specific heat of $NpCoGa_5$ near T_N in applied magnetic fields.

to 70 K is probably due to magnetic fluctuations in a limited temperature region above T_N.

Figure 9 shows the influence of the external applied field on the magnetic phase transition at 47 K. A small field of 1 *T* leaves the transition rather sharp and shifts it slightly to lower temperatures, as expected for an antiferromagnet and in agreement with the magnetization data in Fig. 4. In a field of 2 *T*, the transition is further shifted lower and becomes less pronounced. An additional anomaly arises around 43.5 K. It is presumably connected with the increase of magnetization and the resistivity drop. With further field increase, the anomaly at the ordering temperature around 46 K becomes more and more smeared out, but does not shift further to lower temperature. The second anomaly gradually shifts lower and becomes less pronounced. It can be still seen in 3 *T* around 38 K. In fields above 5 *T*, further increase of the field causes a shift of the magnetic entropy to higher temperature (above T_N). This could be an indication of a ferromagnetic component of the Np magnetic moments that arise in magnetic field.

D. Mössbauer spectroscopy

The ^{237}Np Mössbauer measurements were carried out at different temperatures between 4.2 K and 60 K. Typical Mössbauer spectra are shown in Fig. 10. The 4.2 K spectrum can be well analyzed in terms of an unique set of hyperfine parameters with the magnetic field B_{hf} collinear to the main component V_{zz} of the electric field gradient [$B_{\mathrm{hf}}=180(2)T$; $(eV_{zz}Q)_{\mathrm{eff}}=-3.4(2)$ mm/s]. Upon warming the sample the spectra can still be analyzed, at least up to 32 K, assuming an effective field Hamiltonian and a single set of parameters. Above that temperature severe line broadenings are observed and close to the ordering temperature of $T_N=46.5(5)$ K a single pattern is unable to reproduce the experimental data. Above T_N, the Mössbauer spectra consist of poorly resolved quadrupole patterns of axial symmetry [$|eV_{zz}Q|=3.5(5)$ mm/s]. The isomer shift δ_{IS} of 6.8(2) mm/s relative to $NpAl_2$ is very close to the one found in $NpGa_3$ [$\delta_{\mathrm{IS}}=5.9(1)$ mm/s].[18] This suggests that the Np ions are in a trivalent state (Np^{3+}).

The severe line broadening observed above 32 K can be accounted for by the so-called Wegener relaxation model[19,20]

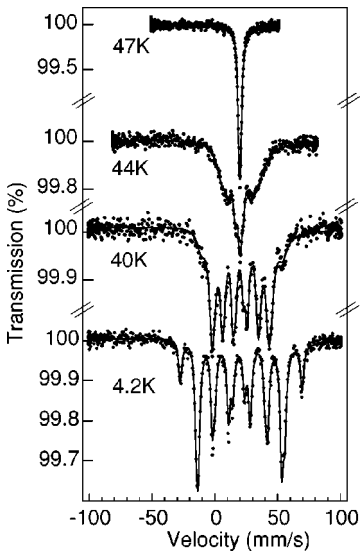

FIG. 10. Mössbauer spectra of $NpCoGa_5$ at different temperatures. The solid lines represent the best fits to the data.

which assumes longitudinal fluctuations of the hyperfine field ($B_{\mathrm{hf}}=\langle B_{\mathrm{hf}}\rangle+B_f(t)$) around a time averaged value $\langle B_{\mathrm{hf}}\rangle$. The linewidths are then given by

$$W=W_0+2\gamma_L(m_e,m_g), \tag{7}$$

where W_0 is the linewidth in the absence of relaxation broadening and

$$\gamma_L(m_e,m_g)=(g_e m_e-g_g m_g)^2\mu_N^2\langle B_f^2\rangle\tau_c\hbar^{-1}. \tag{8}$$

g_e, g_g, m_e, m_g are the nuclear g factors and the magnetic quantum numbers of the excited and ground state respectively; τ_c is the longitudinal correlation time. All spectra at $T\geqslant 32$ K were analyzed in the frame of this model by constraining the intrinsic linewidth W_0 to the value of 3.2 mm/s observed at 4.2 K. In a very narrow temperature range close to T_N ($44\leqslant T<T_N$) one observes the coexistence of a magnetic and a paramagnetic component. The paramagnetic fraction (about 10% at 44 K) grows at the expense of the magnetic one when increasing the temperature. The temperature dependences of $\langle B_{\mathrm{hf}}\rangle$ and of $\Delta=2\mu_N^2\langle B_f^2\rangle\tau_c\hbar^{-1}$ responsible for the line broadenings are presented in Fig. 11 [$(eV_{zz}Q)_{\mathrm{eff}}$

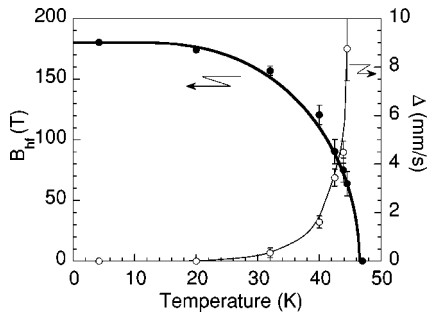

FIG. 11. Temperature dependence of the hyperfine field (full circles) and of the relaxation broadening parameter Δ (open circles) in $NpCoGa_5$. The thick line is a fit of $B_{\mathrm{hf}}(T)$ to a $J=\frac{1}{2}$ Brillouin curve whereas the thin line, $\Delta(T)$, is only a guide to the eye.

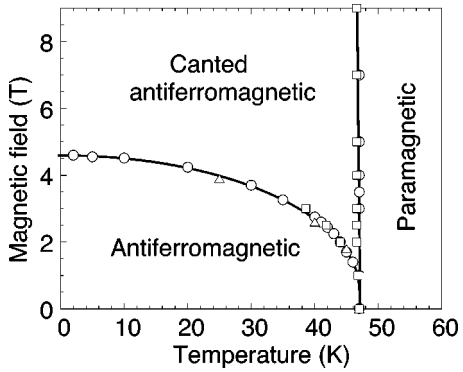

FIG. 12. Magnetic phase diagram of $NpCoGa_5$ as inferred from magnetization (circles), resistivity (triangles), and specific heat (squares) measurements.

is basically temperature independent in the ordered state]. The hyperfine field was shown to follow a $J=\frac{1}{2}$ Brillouin behavior. This indicates that the ground state is a doublet, in agreement with the magnetic entropy released at T_N ($\sim R \ln 2$). From the hyperfine field of 180 *T* measured at 4.2 K, one deduces that the Np^{3+} ions carry an ordered neptunium moment of 0.84(5) μ_B at saturation. The fact that the quadrupolar interaction measured in the ordered and paramagnetic states are about the same suggests that the Np moments are aligned along the tetragonal *c*-axis which is the main component of the electric field gradient in the paramagnetic state.

IV. DISCUSSION

Magnetization, resistivity, specific-heat, and Mössbauer measurements are complementary and show remarkable agreement. From these data, the magnetic phase diagram of $NpCoGa_5$ can be drawn (Fig. 12).

The observation of a positive Curie temperature ($\theta_p \approx 42$ K) within a quasi-2D structure ($NpCoGa_5$ can be viewed as alternating layers of $NpGa_3$ and $CoGa_2$ stacked along the tetragonal *c*-axis) suggests that the zero-field magnetic structure of $NpCoGa_5$ consists of ferromagnetic basal planes stacked antiferromagnetically (notice that $NpGa_3$ is a ferromagnet below 50 K). The simplest magnetic structure compatible with these views is the one observed in isostructural $UPtGa_5$[21] and $UPdGa_5$[22] by neutron diffraction. However, at this stage a more complex structure cannot be excluded.

The exact nature of the high-field magnetic phase of $NpCoGa_5$ remains unclear. Actually, the field induced transition observed by magnetization does not correspond to a clear step within a narrow range of field as usually observed for metamagnetism but rather consists of a broad, nonfinishing transition. Accordingly, the $M(T)$ curves are changing very progressively as the magnetic field is increased, without a clear demarcation between the low-field antiferromagnetic-like transition and the high-field ferromagnetic-like increase. Similarly, the resistivity as a function of the magnetic field is continuously decreasing instead of simply displaying a peak at the critical field. From these observations, we tentatively infer that a ferromagnetic contribution develops in the initial antiferromagnetic structure through the rotation of magnetic moments leading to a canted antiferromagnet structure type.

A phenomenological approach to explain this behavior would be to compare $NpCoGa_5$ with UPdSn, for which M(B)[23] and ρ(B)[24] data are quite similar to those presented here, and for which the magnetic structure was determined by neutron diffraction.[25] UPdSn is an antiferromagnet but a 3.5*T* magnetic field induces a spin-flop transition from antiferromagnetism to canted antiferromagnetism by the rotation of one magnetic moment whereas the four other moments of the magnetic cell remain unchanged. By analogy to the above-mentioned structure of UPdSn, one may speculate that the high-field magnetic phase of $NpCoGa_5$ could well be a canted antiferromagnet resulting from the rotation of whole or part of the magnetic moments.

The structural similarity between $NpCoGa_5$ and $NpGa_3$ has already been pointed out. The $NpGa_3$ units in $NpCoGa_5$ are very close to pure $NpGa_3$ both in the Np–Ga–Np bond angles, 90° ($NpGa_3$) and 90° and 90.35° ($NpCoGa_5$), and in the Np–Ga interatomic distances, 12×3.007 Å for $NpGa_3$ and 4×2.996 Å (Np-Ga($1c$)) and 8×2.987 Å (Np-Ga($4i$)) for $NpCoGa_5$. Contrarily to the behavior observed in $CeRhIn_5/CeIn_3$,[26] the differences in the magnetic properties between $NpCoGa_5$ and $NpGa_3$ cannot be explained as simply due to a chemical pressure effect. $NpGa_3$ can be considered as a quasi-localized $5f$ electron system.[18] This was confirmed from the pressure dependences of both the Np ordered moment ($\sim -5.6\times 10^{-3}$ μ_B/GPa) and of the ordering temperature (~4.1 K/GPa).[27] For $NpCoGa_5$, T_N increases only slightly with pressure (~0.4 K/GPa) and the ordered Np moment (0.84 μ_B) as well as the value of T_N (47 K) are significantly reduced in comparison to those observed in $NpGa_3$ (1.56 μ_B and 65 K, respectively[18]). As shown recently by a simple tight-binding model, applied to the $UMGa_5$ series, *f-p* hybridization and *f-d* hybridization play a dominant role in determining the relative trends in these materials.[28] Similar hybridization effects could explain the lowering of T_N and of the Np ordered moment in $NpCoGa_5$ which can thus be classified as a moderately delocalized $5f$-electron system.

The comparison of the magnetic and electronic properties of $NpCoGa_5$ with its well-known plutonium counterpart is also interesting. Whereas superconductivity appears at $T_c = 18.5$ K in $PuCoGa_5$, an antiferromagnetic order develops below $T_N = 47$ K in $NpCoGa_5$. The Sommerfeld specific heat coefficients of $NpCoGa_5$ ($\gamma = 64$ mJ mol^{-1} K^{-2}) and of $PuCoGa_5$ ($\gamma = 77$ mJ mol^{-1} K^{-2}) are comparable and much higher than in the Pauli paramagnet $UCoGa_5$ ($\gamma = 4$ mJ mol^{-1} K^{-2}). We may deduce that similar densities of states at the Fermi energy arise in both Pu and Np compounds. However, it should be mentioned that band-structure calculations infer similar Fermi surfaces for $NpCoGa_5$ and $UMGa_5$, on one hand, and for $PuCoGa_5$ and Ce*M*In_5 on the other hand.[14] The experimental evidence that the neptunium valence is Np^{3+} in $NpCoGa_5$ is a key issue of our work because the one to one similarity noted above can be understood by the difference in *f*-electron number based on the *j-j* coupling scheme discussed by Hotta and Ueda.[29]

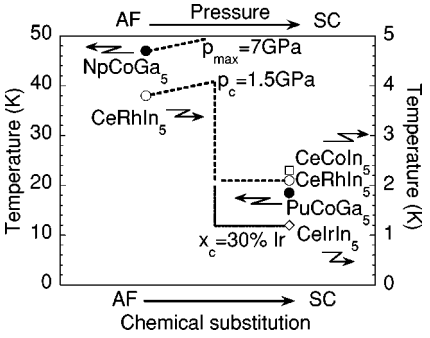

FIG. 13. Schematic diagram of the magnetic and superconducting $AnCoGa_5$ and $CeMIn_5$ systems. The vertical scale represents the Néel or superconducting critical temperature. The left-hand-side scale of temperature applies for $AnCoGa_5$ compounds whereas the right-hand-side scale (ten times smaller) applies for $CeMIn_5$. The dashed lines represent either the application of pressure (slightly increasing the Néel temperatures of $NpCoGa_5$ and $CeRhIn_5$ and turning the latter to a superconductor above $p=1.5$ GPa) or the chemical substitution of Rh by Ir in the $CeRh_{1-x}Ir_xIn_5$ solid solution (bulk superconductivity appears for $x \geqslant 0.3$). The acronyms "AF" and "SC" stand for "antiferromagnetism" and "superconductivity," respectively.

Another strong analogy can be drawn with the isostructural $CeMIn_5$ (M=Rh,Ir,Co) system where unconventional superconductivity develops in proximity to antiferromagnetic order.[30] In $CeRhIn_5$, an applied pressure of 1.5 GPa suffices to induce a first-order-like transition from the antiferromagnetic ($T_N \approx 4$ K) to the superconducting state ($T_c \approx 2.1$ K).[26] Our resistivity measurements under pressure did not reveal any such transition in $NpCoGa_5$ up to $p=7$ GPa. However, the slight and regular increase of the Néel temperature of $NpCoGa_5$ with pressure recalls the $CeRhIn_5$ behavior observed up to $p_c=1.5$ GPa. Taking into account that the Néel and critical temperatures are one order of magnitude higher in $NpCoGa_5$ and $PuCoGa_5$ than in $CeRhIn_5$, an antiferromagnetic/superconductor transition in $NpCoGa_5$ at a significantly higher pressure than 1.5 GPa or even 7 GPa cannot be excluded. Figure 13 presents a schematic comparison of the $CeMIn_5$ and $AnCoGa_5$ systems and the influence of pressure on their magnetic and electronic behavior. The figure also shows that another way to tune the antiferromagnetic $CeMX_5$ systems to superconductivity is chemical substitution. Indeed, the substitution of 30% of Rh atoms by Ir in $CeRhIn_5$ is sufficient to induce superconductivity, which coexists with antiferromagnetism up to 70% of Ir. Above this Ir concentration, the antiferromagnetic order vanishes and only superconductivity is observed.[31] By analogy, an antiferromagnetic/superconductor transition may be anticipated in the diluted system $(Np_xPu_{1-x})CoGa_5$, possibly with coexistence of both antiferromagnetism and superconductivity unless an intermediate, non-superconducting paramagnetic state occurs between the pure neptunium and plutonium systems.

V. CONCLUSION

$NpCoGa_5$ has been shown to order antiferromagnetically below 47 K by magnetization, resistivity, specific heat, and Mössbauer measurements. The latter technique indicates that the Np ions are trivalent and carry a moment of 0.84 μ_B. The observation of a positive Curie temperature together with the 2D nature of the crystal structure suggests that the magnetic structure of $NpCoGa_5$ consists of ferromagnetic basal planes stacked along the c-axis. A field-induced magnetic transition was shown to set in at moderate applied fields ($B_c \approx 4T$ at $T=5$ K). This new phase is probably a canted antiferromagnet whose ferromagnetic component results from a rotation of the moments. Further investigations by neutron or resonant x-ray diffraction (magnetic structure) will be required to confirm and determine more precisely these magnetic structures. Comparisons with the parent $NpGa_3$ compound suggests that $NpCoGa_5$ is a moderately delocalized $5f$-electron system. There appears a strong analogy between $AnCoGa_5$ and $CeMIn_5$. Although $NpCoGa_5$ does not show any hint of superconductivity down to $T=0.4$ K, it appears to be, with a comparable Sommerfeld specific heat-coefficient, close to $PuCoGa_5$ but on the "antiferromagnetic side" of the superconducting/magnetic border.

ACKNOWLEDGMENTS

We are grateful to J. D. Thompson, G. H. Lander, and H. v. Löhneysen for fruitful discussions. P.J. acknowledges the European Commission for support in the frame of the "Training and Mobility of Researchers" program. The high purity Np metals required for the fabrication of the compound were made available through a loan agreement between Lawrence Livermore National Laboratory and ITU, in the frame of a collaboration involving LLNL, Los Alamos National Laboratory and the U.S. Department of Energy.

[1] F. Steglich, J. Aarts, C. D. Bredl, W. Lieke, D. Meschede, W. Franz, and H. Schäfer, Phys. Rev. Lett. **43**, 1892 (1979).

[2] H. R. Ott and Z. Fisk, in *Handbook on the Physics and Chemistry of the Actinides*, edited by A. J. Freeman and G. H. Lander (North-Holland, Amsterdam, 1987), Vol. 5, p. 85.

[3] A. Amato, Rev. Mod. Phys. **69**, 1119 (1997).

[4] S. S. Saxena, P. Agarwal, K. Ahilan, F. M. Grosche, R. K. W. Hasselwimmer, M. J. Steiner, E. Pugh, I. R. Walker, S. R. Julian, P. Monthoux, G. G. Lonzarich, A. Huxley, I. Sheikin, D. Braithwaite, and J. Flouquet, Nature (London) **406**, 587 (2000).

[5] D. Aoki, A. Huxley, E. Ressouche, D. Braithwaite, J. Flouquet, J. P. Brison, E. Lhotel, and C. Paulsen, Nature (London) **413**, 613 (2001).

[6] J. Bardeen, L. N. Cooper, and J. R. Schrieffer, Phys. Rev. **108**, 1175 (1957).

[7] J. L. Sarrao, L. A. Morales, J. D. Thompson, B. L. Scott, G. R. Stewart, F. Wastin, J. Rebizant, P. Boulet, E. Colineau, and G. H. Lander, Nature (London) **420**, 297 (2002).

[8] F. Wastin, P. Boulet, J. Rebizant, E. Colineau, and G. H. Lander, J. Phys.: Condens. Matter **15**, 2279 (2003).
[9] I. Opahle and P. M. Oppeneer, Phys. Rev. Lett. **90**, 157001 (2003).
[10] S. Noguchi and K. Okuda, J. Magn. Magn. Mater. **104–107**, 57 (1992).
[11] C. K. Fair, ''Molen Users Manual—An interactive intelligent system for crystal structure analysis,'' Delft. Netherlands, 1989.
[12] J. Rodriguez-Carvajal, Physica B **192**, 55 (1993).
[13] J.-C. Griveau, F. Wastin, and J. Rebizant, Acta Phys. Pol. B **34**, 1319 (2003).
[14] T. Maehira, T. Hotta, K. Ueda, and A. Hasegawa, Phys. Rev. Lett. **90**, 207007 (2003).
[15] N. H. Andersen, in *Crystalline Electric Field and Structural Effects in f-electron Systems*, edited by J. E. Crow, R. P. Guertin, and T. W. Mihalisin (Plenum, New York, 1980), p. 373.
[16] K. Kadowaki and S. B. Woods, Solid State Commun. **58**, 507 (1986).
[17] N. H. Andersen, H. Smith, Phys. Rev. B **19**, 384 (1979).
[18] M. N. Bouillet, T. Charvolin, A. Blaise, P. Burlet, J. M. Fournier, J. Larroque, and J. P. Sanchez, J. Magn. Magn. Mater. **125**, 113 (1993).
[19] H. Wegener, Z. Phys. **186**, 498 (1965).
[20] H. Wegener, in *Proceddings of the International Conference On Mössbauer Spectroscopy,Cracow, Poland*, edited by A. Z. Hrynkiewicz and J. Sawicki (Akademia Gorniczo-Hutnicza Im, S. Staszika W. Krakovie, Cracow, 1975), Vol. 2, p. 257.
[21] K. Kaneko, N. Metoki, N. Bernhoeft, G. H. Lander, Y. Ishii, S. Ikeda, Y. Tokiwa, Y. Haga, and Y. Onuki, Phys. Rev. B **68**, 214419 (2003).
[22] S. Ikeda, N. Metoki, Y. Haga, K. Kaneko, T. D. Matsuda, A. Galatanu, and Y. Onuki, J. Phys. Soc. Jpn. **72**, 2622 (2003).
[23] F. R. de Boer, E. Brück, H. Nakotte, A. V. Andreev, V. Sechovsky, L. Havela, P. Nozar, C. J. M. Denissen, K. H. J. Buschow, B. Vaziri, M. Meissner, H. Maletta, and P. Rogl, Physica B **176**, 275 (1992).
[24] F. Honda, A. Alsmadi, H. Nakotte, J. Kamarad, V. Sechovsky, A. H. Lacerda, and M. Mihalik, Acta Phys. Pol. B **34**, 1197 (2003).
[25] H. Nakotte, R. A. Robinson, A. Purwanto, Z. Tun, K. Prokes, E. Bruck, and F. R. de Boer, Phys. Rev. B **58**, 9269 (1998).
[26] H. Hegger, C. Petrovic, E. G. Moshopoulou, M. F. Hundley, J. L. Sarrao, Z. Fisk, and J. D. Thompson, Phys. Rev. Lett. **84**, 4986 (2000).
[27] S. Zwirner, V. Ichas, D. Braithwaite, J. C. Waerenborgh, S. Heathman, W. Potzel, J. C. Spirlet, J. Rebizant, and G. M. Kalvius, Phys. Rev. B **54**, 12283 (1996).
[28] N. O. Moreno, J. L. Sarrao, M. F. Hundley, J. D. Thompson, and Z. Fisk (unpublished).
[29] T. Hotta and K. Ueda, Phys. Rev. B **67**, 104518 (2003).
[30] C. Petrovic, R. Movshovich, M. Jaime, P. G. Pagliuso, M. F. Hundley, J. L. Sarrao, Z. Fisk, and J. D. Thompson, Europhys. Lett. **53**, 354 (2001).
[31] P. G. Pagliuso, C. Petrovic, R. Movshovich, D. Hall, M. F. Hundley, J. L. Sarrao, J. D. Thompson, and Z. Fisk, Phys. Rev. B **64**, 100503 (2001).